Title: Sex differences in central amygdala glutamate responses to calcitonin gene-related peptide

Abbreviated title: Sex differences in CeLC glutamate response to CGRP

Author Names and Affiliations: Rebecca Lorsung[1], Nathan Cramer[1,2], Jason Bondoc Alipio[1], Yadong Ji[3], Sung Han[4], Radi Masri[2,3], Asaf Keller[1,2]

[1]Department of Neurobiology, School of Medicine, University of Maryland, Baltimore, Maryland 21201, USA.

[2]Center to Advance Chronic Pain Research, University of Maryland School of Medicine, Baltimore, MD 21201, USA

[3]Department of Advanced Oral Sciences and Therapeutics, School of Dentistry, University of Maryland, Baltimore, Maryland 21201, USA, and Faculty of Dentistry, University of Jordan, Amman, Jordan.

[4]Peptide Biology Laboratory, The Salk Institute for Biological Studies, La Jolla, CA 92037, USA

Conflict of Interest Statement: The authors declare they have no conflicts of interest to disclose.

Acknowledgments:

This work was supported by National Institutes of Health–National Institute of Neurological Disorders and Stroke Grants R01NS099245, R01NS069568, R01NS127827 and Fellowship F31NS134126 (to RL).

Dr. Jason Alipio performed work on this project while in the Department of Neurobiology. He is currently affiliated with the Center for Regenerative Medicine, Massachusetts General Hospital, Boston, MA, USA. 02118

Abstract

Women are disproportionately affected by chronic pain compared to men. While societal and environmental factors contribute to this disparity, sex-based biological differences in the processing of

pain are also believed to play significant roles. The central lateral nucleus of the amygdala (CeLC) is a key region for the emotional-affective dimension of pain, and a prime target for exploring sex differences in pain processing since a recent study demonstrated sex differences in CGRP actions in this region. Inputs to CeLC from the parabrachial nucleus (PB) play a causal role in aversive processing, and release both glutamate and calcitonin gene-related peptide (CGRP). CGRP is thought to play a crucial role in chronic pain by potentiating glutamatergic signaling in CeLC.

However, it is not known if this CGRP-mediated synaptic plasticity occurs similarly in males and females. Here, we tested the hypothesis that female CeLC neurons experience greater potentiation of glutamatergic signaling than males following *endogenous* CGRP exposure. Using trains of optical stimuli to evoke transient CGRP release from PB terminals in CeLC, we find that subsequent glutamatergic responses are preferentially potentiated in CeLC neurons from female mice. This potentiation was CGRP-dependent and involved a postsynaptic mechanism. This sex difference in CGRP sensitivity may explain sex differences in affective pain processing.

Significance statement

The central lateral nucleus of the amygdala (CeLC) receives a dense projection from parabrachial nucleus (PB) neurons that corelease calcitonin gene-related peptide (CGRP) and glutamate following aversive stimuli. This PB_{CGRP}→CeLC projection plays a causal role in chronic pain. We show that endogenous CGRP release potentiates glutamate signaling in female, but not male, CeLC neurons. In the context of previous work in male CeLC, this suggests that that females are more sensitive to even transient CGRP release events. Understanding how this sex difference in CGRP sensitivity arises could enhance strategies for treating chronic pain in both women and men.

Introduction

Women are disproportionately affected by pain, experiencing greater severity, duration, and incidence of chronic pain across many conditions (Mogil, 2009, 2012, 2021; Osborne and Davis, 2022). While societal and environmental factors can influence this sex bias (Fillingim, 2000; Bartley and Fillingim, 2013), genetic, neuroimmune and neurobiological components are thought to be involved in these sex differences (Stratton et al., 2024). Identifying mechanisms that drive sex differences in chronic pain may aid in the development of novel diagnostics and therapies to better treat women and men with these conditions.

The central lateral nucleus of the amygdala (CeLC; the "nociceptive amygdala") is a critical center for the emotional-affective dimension of pain (Neugebauer et al., 2020). Nociceptive inputs to CeLC originate primarily from parabrachial nucleus, whose afferents form large—presumably highly efficacious—perisomatic synapses in CeLC (Delaney et al., 2007; Chou et al., 2022). CeLC integrates nociceptive and aversive inputs (Neugebauer et al., 2003; Neugebauer, 2015) , and interacts with other key nodes in the pain system (Janak and Tye, 2015; Neugebauer et al., 2020). That parabrachial nucleus inputs to CeLC are causally related to persistent pain is supported by studies showing that pain-like behaviors can be suppressed by manipulating this pathway (Neugebauer, 2015; Wilson et al., 2019; Chiang et al., 2020; Raver et al., 2020; Mazzitelli et al., 2021).

Parabrachial nucleus (PB) neurons that project to CeLC express both glutamate and calcitonin gene related peptide (CGRP) (Shimada et al., 1985; Schwaber et al., 1988; Neugebauer et al., 2020). While low-frequency firing predominantly facilitates glutamate signaling, high-frequency firing of PB CGRP neurons induces the fusion of large dense core vesicles (LDCVs) (Tallent, 2008; Schöne et al., 2014; Qiu et al., 2016), releasing packaged neuropeptides including CGRP. PB neurons which express CGRP fire at these high frequencies in response to aversive input, especially in chronic pain conditions (Uddin et al., 2018; Raver et al., 2020; Smith et al., 2023). The subsequent release of CGRP upon CeLC neurons is causally

related to chronic pain conditions (Han et al., 2005, 2010; Okutsu et al., 2017; Shinohara et al., 2017; Chou et al., 2022; Kang et al., 2022; Presto and Neugebauer, 2022; Allen et al., 2023; Kim et al., 2024).

Despite known sex differences in pain conditions and in pain mechanisms, including sex differences in CGRP-related pain mechanisms in humans (Labastida-Ramírez et al., 2019; de Vries Lentsch et al., 2021), essentially all data on PB and its effects on CeLC are from studies of male animals. An important exception is a demonstration that CGRP RNA levels in the CeLC are upregulated at different stages of neuropathic pain in male and female rats, and that CGRP receptor antagonist has sex-specific effects on pain behaviors (Presto and Neugebauer, 2022). Also relevant is a finding that the effects of CGRP on GABA transmission in spinal cord, and on pain behaviors, is sex-specific (Paige et al., 2022).

Here, we test the hypothesis that CGRP exerts a sex-dependent effect on glutamate signaling in the CeLC. By using a model system which combines optogenetics with patch electrophysiology, we evoke *endogenous* CGRP release from PB_{CGRP} terminals in the CeLC ***in vitro***. By relying on endogenous release of CGRP, rather than exogenous application of CGRP, we minimize the risk of off target effects by more closely mimicking physiologic release of neuropeptides. We first validate that single optic stimulation of channel rhodopsin (ChR2) expressing PB_{CGRP} terminals induces glutamate release in the CeLC, while high frequency stimulation is required to induce neuropeptide release ***in vitro***. We then test the effect of endogenously released CGRP on glutamate signaling. We predicted that CeLC glutamate signaling is potentiated by CGRP signaling, in line with previous studies in male rodents (Han et al., 2010; Okutsu et al., 2017), in both sexes, but with a greater magnitude of potentiation in female neurons.

Methods:

Animals

All procedures adhered to the Guide for the Care and Use of Laboratory Animals and approved by the Institutional Animal Care and Use Committee at the University of Maryland School of

Medicine. We used 25 CGRP (calcitonin-gene-related peptide)-CRE heterozygous mice (13 female, 12 male) that were bred in house from male B6.Cg-Calca$^{tm1.1(cre/EGFP)Rpa}$/J (stock #033168) x female C57BL/6J mice (strain #000664). Breeding pairs were obtained from The Jackson Laboratory. Offspring were weaned at postnatal day (PD)21 and housed two to five per cage in single-sex groups. Food and water were available ad libitum, and lights were maintained on a 12/12 h light/dark cycle. Two males (M1-2) and two females (F1-2) were used for fiber photometry experiments. The remaining mice were used for ***in vitro*** electrophysiology, where 1-3 neurons were recorded in each mouse from 1-3 CeLC slices.

Virus injection

We anesthetized the animals with isoflurane and placed them in a stereotaxic frame. Either left or right PBN (-5.2 mm AP, ±1.5 mm ML, -2.9 mm DV) was targeted via a small craniotomy (~1-2 mm). Only the right PBN was targeted in LDCV photometry recordings. We injected 0.5 µL of adeno-associated virus generated by the University of Maryland School of Medicine's Viral Vector Core – Baltimore, Maryland; AAV5-DIO-ChR2-eYFP, OR 0.25 µL AAV_{DJ}-DIO-CYbSEP2 co-injected with AAV5-DIO-ChR2-eYFP. CybSEP2 is a presynaptic pH-sensitive presynaptic sensor which is trafficked by LDCVs, and which undergoes a shift in fluorescence upon LDCV fusion and neuropeptide release (Kim et al., 2024). Viruses were injected using a MICRO2T SMARTouch™ controller and Nanoliter202 injector head (World Precision Instruments) at a flow rate of 100 nL/min. The pipette was left in place for 10 min before being slowly retracted over 5–10 min. Mice were given Rimadyl for postoperative analgesia. Injection sites were verified by visually confirming robust eYFP fluorescence in the external PBN.

112

113 In vitro slice electrophysiology

114 We anesthetized adult mice (2 – 12 months old) generated live brain slices from adult mice and
115 generated 300µm thick coronal sections through the central nucleus of the amygdala using a
116 modified slice collection method as described in (Ting et al., 2014) and our prior studies. For
117 recordings, we placed slices in a submersion chamber continuously perfused (2 mL/min) with
118 artificial cerebrospinal fluid (ACSF): 119 mM NaCl, 2.5 mM KCl, 1.2 mM NaH_2PO_4, 2.4 mM
119 $NaHCO_3$, 12.5 mM glucose, 2 mM $MgSO_4 \cdot 7H_2O$, and 2 mM $CaCl_2 \cdot 2H_2O$. ACSF was adjusted to a
120 pH of 7.4, mOsm of 305, and bubbled with carbogen (95% O_2 and 5% CO_2) throughout use.

121

122 We obtained whole-cell voltage-clamp recordings (−70 mV) from the capsular region of the CeLC
123 using borosilicate pipettes with an impedence of 4-6 MΩ and containing: 130 mM cesium
124 methanesulfonate, 10 mM HEPES, 1 mM magnesium chloride, 2.5 mM ATP-Mg, 0.5 mM EGTA,
125 0.2 mM GTP-Tris, 5 mM QX-314, and 2% biocytin (pH of 7.3, 285 mOsm). Excitatory postsynaptic
126 currents (EPSCs) were optically evoked by whole field illumination at 470 nm (Lambda LS light
127 source, Sutter Instrument) and maximum power of 1.4 mW . Optical stimulation parameters,
128 both high frequency stimulation (10 or 20 Hz, 3 ms pulse duration) and single/paired exposures
129 (3 ms pulse duration, 100 ms interval), were controlled by a SmartShutter system (Sutter
130 Instrument). We monitored series resistance by measuring the current evoked by a -5 mV square
131 pulse at ~ 20s intervals. Evoked oEPSC amplitudes were quantified using Clampfit 11.2
132 (Molecular Devices).

133

In vitro LDCV quantification

Acute brain sections containing the CeLC were collected as above (see "In vitro slice electrophysiology") from adult mice previously injected with AAV_{DJ}-DIO-CYbSEP2 (Kim et al., 2024) and AAV5-DIO-ChR2-eYFP in the ipsilateral parabrachial nucleus. A fiber optic probe (400 µM diameter, 0.39 NA; RWD Life Sciences) was placed over the visually identified fluorescent afferents from PB within CeLC to record LDCV sensor transients evoked by high frequency optical stimulation of PB_{CGRP} fibers in the CeLC at 470 nm (CoolLED). Sensor transients were recorded through the fiber optic probe connected to a RZX10 LUX fiber photometry processor running Synapse software (Tucker-Davis Technologies) through a Doric mini cube (Doric Lenses). Fiber photometry LED power was calibrated to 15 µW using a digital optical power meter (Thor Labs).

We analyzed the data using customized Python scripts adapted from Tucker-Davis Technologies templates which calculated relative changes in fluorescence. Changes in sensor fluorescence were calculated by subtracting the scaled isosbestic signal (405 nm) from the sensor fluorescence (465 nm). Event related changes in sensor fluorescence were converted to ΔF/F using the 5 second window prior to each stimulation as baseline. The area under the curve (AUC) for the average response was calculated for each mouse using the AUC analysis function in GraphPad Prism.

Experimental Design and Statistical Analysis:

Statistical tests were conducted using Prism 10 (GraphPad), and sample size was determined using G*Power software suite (Heinrich-Heine, Universität Düsseldorf). Parametric tests were used when appropriate assumptions were met; otherwise, we used nonparametric tests. Specific

155 statistical tests are detailed in Table 1. Unless describing a time course, baseline vs post optic
156 comparisons are shown as the average in the 90 seconds before and 90 seconds after optic tetanus
157 delivery. Averages described in the text are formatted as mean ± SD unless otherwise stated. All
158 figures were designed using a combination of Prism 10 (GraphPad) and Inkscape 1.3.2. Atlas
159 images for Figure 5A were adapted from (Franklin and Paxinos, 2008), and accessed via a web
160 based tool (https://labs.gaidi.ca/mouse-brain-atlas/).

161

Table 1: Statistics for showing the corresponding figure number, animals, metric, comparisons being made, test statistic, medians or means, sample size, and p values

Figure	Animals	Metric	Comparison	Test Statistic	Mean	Sample size	p Value
2C	F3-13, M3-7	Normalized oEPSC amplitude	CGRP vs Baseline within sex	Female paired t test (t=4.971, df=15) Male paired t-test (t=0.5583, df=7)	Female: Baseline 1.00, CGRP 1.36 Male: Baseline 1.00, CGRP 1.06	16 female neurons, 8 male neurons	Female: p=0.0002, Male: p=0.59
2D	F3-13, M3-7	Normalized oEPSC amplitude	Sex, Time, Sex x Time	RM Mixed-effects analysis Sex (F (1, 314) = 9.794), Time (F (6.229, 139.7) = 2.629), Sxt (F (14, 314) = 2.080) Dunnet's multiple comparison test performed vs baseline average (α= 0.05)	Timepoint from left to right, 0.05 Hz sampling (m, f): Baseline 1) 0.86, 0.97 2) 0.99, 1.18 3) 1.00, 1.05 4) 0.98, 0.99 5) 0.90, 0.94 6) 0.84, 1.12 7) 08.56, 1.01 8) 1.03, 1.00 9) 1.07, 0.924 10) 1.34, 0.91 CGRP 1) 1.26, 1.53 2) 0.89, 1.45 3) 0.97, 1.32 4) 0.89, 1.17 5) 0.74, 1.00	8 male neurons, 15 female neurons	Sex: p <0.01 Time: p = 0.02 SxT: p=0.01
2E	F3-13, M3-12	Normalized baseline holding current	After vs before within sex	Female paired t-test (t=2.267, df=14), Male Wilcoxon test (W=54.00)	Female: Before 1.00, After -1.52 Male: Before 1.00, After 3.22	15 female neurons, 15 male neurons	Female: p=0.04, Male: p =0.14
2F	M8-12	Normalized oEPSC amplitude	CGRP vs baseline	Paired t test (t=0.5971, df=6)	Male: Baseline 1.00, CGRP 0.90	7 male neurons	

2G	M8-12	Normalized oEPSC amplitude	Time	RM Mixed effects analysis Time (F (2.203, 12.75) = 0.6122), Dunnet's multiple comparison test performed vs baseline average (α= 0.05)	Timepoint from left to right, 0.033 Hz sampling: Baseline 1) 1.00 2) 0.98 3) 1.00 4) 0.86 5) 1.38 6) 1.14 7) 1.03 8) 0.87 9) 0.91 10) 1.08 CGRP 1) 0.92 2) 0.90 3) 0.91 4) 0.95 5) 0.73	7 male neurons	P=0.57
2H	F3-13, M3-12	Response magnitude (>20% for increased/decreased)	Male vs female CeLC neurons	Fisher's exact test	N/A	15 male neurons, 16 female neurons	P=0.0032
3A	F3-4, 6-8, 9-10	oEPSC amplitude normalized to baseline	Between treatments	Paired t test (t=0.5296, df=7)	$CGRP_1$: 1.533 $CGRP_2$: 1.472	8 female neurons	P=0.61
3B	F4, 6, 8-9, 11-12	oEPSC amplitude normalized to baseline	Between treatments	Paired t test (t=2.960, df=7)	$CGRP_1$: 1.545 $CGRP_2$ + Antagonist: 1.149	8 female neurons	P=0.02
3C	F3-4, 6, 8-9, 12-13	Normalized paired pulse ratio (PPR)	Between treatments	Paired t test (t=1.558, df=9)	Baseline: 1 CGRP: 0.847	10 female neurons	P=0.15
4A	F3-13	Normalized potentiation amplitude	Right vs left CeLC (female only)	Unpaired t test (t=0.7812, df=13)	Left: 1.492, Right: 1.360	7 left, 8 right CeLC neurons	P=0.45

4B	F3-13	oEPSC baseline amplitude	Right vs left CeLC (female only)	Unpaired t test (t=0.008863, df=17)	Left: -24.22, Right: -24.15	9 left, 10 right CeLC neurons	p>0.99
4C	F3-13	Baseline Paired pulse ratio (PPR)	Right vs left CeLC (female only)	Unpaired t test (t=0.3136, df=11)	Left: 0.59, Right: 0.55	6 left, 7 right CeLC neurons	P=0.76
4D	F3-9,11-13	Mouse age	Responding vs nonresponding female neurons	Unpaired t test (t=0.2681, df=13)	Non responder: 32.17, responder: 30.54	6 non responder and 9 responder mice	P=0.79
4E	F3-9,11-13	Virus incubation	Responding vs nonresponding female neurons	Mann-Whitney test (U = 15)	Non responder median: 7.14, responder median: 12.57	6 non responder and 9 responder mice	P=0.17
4F	F3-9,11-13	Access resistance	Responding vs nonresponding female neurons	Mann-Whitney test (U=20)	Non responder median: 0.83, responder median: 0.42	5 non responder and 11 neurons	P=0.44
4G	F3-13	Baseline holding current	Responding vs nonresponding female neurons	Mann-Whitney test (U=29)	Non responder median: -37.00 responder median: -38.00	6 non responder and 10 neurons	P=0.96
4H	F3-9,11-13	Membrane resistance	Responding vs nonresponding female neurons	Unpaired t test (t=0.8766, df=13)	Non responder: 947.8, responder median: 685.1	6 non responder and 9 responder mice	P=0.4
4I	F3-9,11-13	Cell capacitance	Responding vs nonresponding female neurons	Unpaired t test (t=0.02697, df=13)	Non responder: 107.1, responder median: 106.1	6 non responder and 9 responder mice	P=0.98
5B	F3-13, M3-12	Proportion patched CeLC neurons	Male vs female	Fisher's exact test	N/A	21 male and 23 female CeLC	P=0.449

		with evoked oEPSCs				neurons patched	
5C	F3-13, M3-12	oEPSC amplitude	Male vs female	Unpaired t test (t=0.05990, df=32)	Male: -24.57, female: -24.19	15 male and 19 female neurons	P=0.95
5D	F3-13, M3-12	Baseline holding current	Male vs female	Mann-Whitney test (U=96)	Male median: -50.0, Female median: -37.90	14 male and 18 female neurons	P=0.27
5E	F3-13, M3-12	Access resistance	Male vs female	Mann-Whitney test (U=104)	Male median: 0.56, Female median: 0.79	14 male and 16 female neurons	P=0.76
5F	F3-9,11-13, M3-12	Membrane resistance	Male vs female	Unpaired t test (t=0.4094, df=30)	Male: 760.1, female: 847.9	15 male and 17 female neurons	P=0.69
5G	F3-9,11-13, M3-12	Cell capacitance	Male vs female	Unpaired t test (t=0.4610, df=30)	Male: 113.1, female: 847.9	15 male and 17 female neurons	P=0.65

Results

High frequency optical stimulation of PB_{CGRP} terminals induces LDCV release in the CeLC

Parabrachial nucleus (PB) neurons that express calcitonin gene-related peptide (CGRP; PB_{CGRP}) co-release glutamate and CGRP. To evoke glutamate and CGRP release from these terminals in CeLC, we injected a Cre-dependent channel rhodopsin (ChR2) virus into the PB of CGRP-Cre mice (Fig. 1A). The CeLC receives dense input from PB CGRP neurons (Fig. 1B), whose cell bodies densely localize in the lateral parabrachial nucleus (LPB, Fig. 1C). We first recorded optically-induced excitatory postsynaptic currents (oEPSCs) from ipsilateral CeLC neurons evoked by a single pulse of 470 nm light (3 msec duration, 0.05 Hz) (Fig.1). Application of AMPA receptor antagonist (CNQX, 20 µM) suppressed oEPSCs, indicating these oEPSCs are dependent on glutamate signaling. Similar suppression was observed in 4 of 4 neurons. While these single

optic stimuli reliably induced oEPSCs in CeLC neurons, high frequency stimulus trains (10 Hz, 5 sec), that mimic firing patterns of PB neurons during noxious stimulation in normal and chronic pain states (Uddin et al., 2018; Raver et al., 2020; Smith et al., 2023), resulted in rapid suppression in oEPSC amplitudes recorded in CeLC neurons from both male and female mice (Fig. 1E, 11 female neurons; 8 male neurons). This suggests that the strength of glutamatergic excitation of CeLC neurons postsynaptic to PB afferents rapidly diminishes during sustained activity.

While high frequency activity causes a drop in glutamatergic drive, we reasoned that these same stimulus trains would be sufficient to drive release of CGRP from large dense core vesicles (LDCVs) (Tallent, 2008; Schöne et al., 2014; Qiu et al., 2016). To test this, we directly measured neuropeptide release from PB_{CGRP} afferents which co-express channelrhodopsin2 (ChR2) and the LDCV sensor CybSEP2. CybSEP2 is a pH sensitive sensor transported by LDCVs, which undergoes a shift in fluorescence upon LDCV fusion and neuropeptide release (Kim et al., 2024). We co-injected Cre-dependent CybSEP2 and Cre-dependent ChR2 into the PB of CGRP-cre mice (Fig. 1A) and performed fiber photometry in slices from ipsilateral CeLC to monitor LDCV release. Figure 1F depicts a heat map obtained from recordings where the duration of the stimulus train increased from 250 ms (5 pulses at 20 Hz) to 10 seconds (200 pulses at 20 Hz). As evidenced by the corresponding ΔF/F (Fig. 1F) and quantified as area under the curve (AUC, Fig. 1G), short duration stimulus trains failed to produce detectable changes in sensor fluorescence. However, increasing the stimulus duration progressively increased recorded fluorescent intensity (Fig. 1G). Similar responses were seen in slices from male and female mice (n = 2). In contrast, mice injected with a single virus, either CybSEP2 (n=1) or ChR2 (n=1), demonstrated no such increase. These data indicate that high frequency optic stimulation is sufficient to induce PB_{CGRP} LDCV fusion, and subsequent neuropeptide release, *in vitro* in the CeLC.

PB glutamatergic signal is potentiated in females following PB endogenous CGRP release

We took advantage of this ability to evoke PB neuropeptide release to determine if endogenous CGRP release potentiates PB_{CGRP}->CeLC glutamatergic synapses. To measure the amplitude of this glutamatergic signaling we recorded responses to single pulses of blue light (3 msec duration, 0.05 Hz) to induce ChR2-mediated glutamatergic oEPSCs in postsynaptic CeLC neurons (Fig. 2). After establishing the baseline oEPSC amplitude, we used high frequency optical stimulation (10 Hz, 5 sec) to evoke neuropeptide release in the CeLC and then remeasured the glutamatergic response to single pulse stimulation. Figure 2A depicts oEPSC recorded from a CeLC neuron from a female mouse, before and after CGRP release, demonstrating a 44% increase in the amplitude of the glutamatergic response after the tetanus stimulation. In contrast, Figure 2B shows that the same procedure failed to potentiate oEPSCs in a CeLC neuron from a male. Group data for female and male mice are quantified in Figure 2C, where CeLC neurons from female mice displayed an average potentiation of 136%±29% ($p=2x10^{-3}$, N=16 cells from 11 female mice) following high frequency tetanus, while male CeLC neurons showed no net potentiation, with an average post-optic tetanus magnitude of 106%±29% (p=0.59, N=8 cells from 5 male mice). The time course of this response is shown in Figure 2D where oEPSCs were significantly potentiated only in female mice (RM two-way mixed-effects sex F (1, 314) = 9.794, p<0.01; time F (6, 229) = 2.629, p=0.02; sex x time F (14, 314) = 2.080, p=0.01), and up to 60 s after the tetanus (Dunnet's multiple comparison test, p<0.05). Additionally, in female CeLC neurons, there was a small reduction of 1.5±2.6 pA in holding current (p=0.04; 15 neurons, 10 mice) in the 5 seconds following high frequency optic tetanus (Fig. 2E). This suggests there was a temporary change in membrane ion conductance induced by the high frequency optic tetanus. In males there was no net change in holding current (p=0.16; 15 neurons, 9 mice, Fig. 2E).

To test whether the observed sex differences in potentiation arise from a higher threshold for potentiation in CeLC neurons from males versus females, we use a higher frequency, longer optical tetanus to encourage greater endogenous CGRP release (20 Hz, 10 sec) while recording from a

population of CeLC neurons patched in separate male mice (N= 7 neurons, 5 mice). In addition, as previous studies demonstrated that CGRP acts through a NMDA-dependent mechanism in the CeLC (Han et al., 2010; Okutsu et al., 2017), we amplified the signal from recruited NMDA channels by excluding Mg^{2+} in the ACSF. Even under these conditions there was no net potentiation in male CeLC neurons, as post-optic tetanus oEPSC amplitude was 89%±46% of baseline (p=0.57, Fig. 2F). Figure 2G depicts the time course of this response (RM one-way mixed-effect of time F(2.203, 12.75)=0.6122, p=0.57).

Across both experiments, only 13% of recorded male CeLC neurons (2/15 neurons, 10 mice) were potentiated (>20% elevation of oEPSC amplitude) following high frequency stimulation. In contrast, potentiation occurred in 62% of female CeLC neurons (10/16 neurons, 11 mice). Figure 2H depicts the responses across all recorded neurons, where male and female CeLC neurons respond differently to high frequency optic stimulation (p=0.003).

Potentiation in females was reproducible within a neuron; once response amplitudes returned to baseline, a similar level of potentiation (p=0.61 compared to the previous potentiation) was achieved by a second delivery of high frequency optic stimulation (N=8 neurons, 5 mice; Fig. 3A). Re-potentiation in female CeLC neurons was suppressed by pre-application of 1 µM of the CGRP receptor antagonist ($CGRP_{8-37}$, p=0.02), suggesting that CGRP signaling contributes to this increase in PB_{CGRP}->CeLC glutamate signaling (N= 8 neurons, 6 mice, Fig. 3B).

Effect of high Frequency optic tetanus on presynaptic release probability and passive membrane properties

We tested whether CGRP dependent potentiation in female neurons is driven by a presynaptic mechanism by comparing oEPSC responses to paired pulse stimulation and calculated a paired pulse ratio (PPR), the ratio of the amplitude of the second pulse divided by the amplitude of the first pulse; changes

in paired pulse ratio implicate the involvement of a presynaptic mechanism (Manabe et al., 1993; Debanne et al., 1996; Dobrunz and Stevens, 1997; Kim and Alger, 2001). A PPR above one is associated with a low probability of vesicle release (i.e., "weaker" synapses), whereas a PPR below one is associated with a high probability of release. Example paired-pulse oEPSCs are shown in Figure 3C (inset). We compared PPR before and after optic tetanus delivery. At baseline, the oEPSC PPR was less than 1 in all female CeLC neurons, suggesting these are high release probability synapses. Female CeLC neurons (10 neurons, 7 mice) did not exhibit a change in PPR following CGRP-mediated potentiation (p=0.15, Fig. 3C). This suggests that CGRP acts postsynaptically.

To test if CGRP mediated potentiation reflects postsynaptic mechanisms, we compared holding current before and after potentiation. While there was a small reduction in holding current in female CeLC neurons immediately following the high frequency optic tetanus (Fig. 2E), there was no change in holding current PB CGRP release compared to baseline in either male (p=0.16; 14 neurons, 9 mice) or female (p=0.21; 16 neurons, 11 mice) CeLC neurons. This suggests that while female CeLC neurons are transiently depolarized in response to high frequency optic tetanus, the potentiated glutamatergic response outlasts the change in driving potential evoked by the tetanus itself. There was no change in series resistance following PB CGRP release in either male (p=0.6; 14 neurons, 9 mice) or female (p=0.62; 16 neurons, 11 mice) CeLC neurons. Therefore, the effects of endogenous CGRP release upon CeLC neurons likely reflect a localized change to the post synapse, and not a more far-reaching alteration to the overall intrinsic membrane properties of the CeLC neurons.

CGRP-dependent potentiation and input strength are consistent between hemispheres and across the A-P axis of the CeLC

Lateralization in the function of CeLC has been reported in several preclinical models of pain (Carrasquillo and Gereau, 2008; Ji and Neugebauer, 2009; Allen et al., 2023). Therefore, we examined whether

lateralization of PB_{CGRP} optic tetanus-evoked potentiation occurs in female neurons. There was no difference (p=0.45; 15 neurons, 10 mice) in potentiation magnitude between left and right CeLC (Fig. 4A). Additionally, there was no difference in baseline oEPSC amplitude (p=0.99; 18 neurons, 12 mice) nor in baseline paired pulse ratio (p=0.76; 18 neurons, 12 mice) between recordings from the left and right CeLC (Fig. 4B-C). These findings indicate that there is no lateralization in PB_{CGRP}->CeLC glutamatergic input strength or synaptic release probability in females.

CeLC may differ functionally not only between hemispheres, but also across the anterior-posterior axis. For example, optogenetic stimulation of PB_{CGRP} inputs to the anterior and posterior CeLC induces different behaviors; stimulating PB_{CGRP} in posterior CeLC inputs induces freezing, while stimulating PB_{CGRP} in anterior CeLC predominantly induces changes in respiration and vasoconstriction (Bowen et al., 2020). Therefore, we compared the sensitivity of the female CeLC across the A-P axis to glutamatergic potentiation following PB CGRP release. In female CeLC neurons where oEPSCs were detected in response to optic stimulation of PB_{CGRP} terminals (direct PB_{CGRP} glutamatergic input), widefield images of the CeLC were acquired following patching. The neuronal anterior-posterior position relative to bregma was then determined using a stereotaxic atlas (Franklin and Paxinos, 2008). The location of recorded neurons was not related to PB CGRP-driven glutamate potentiation (r=0.26, p=0.36; 14 neurons, 8 mice), baseline PB glutamate amplitude (r=0.16, p=0.53; 17 neurons, 10 mice), or baseline PB glutamate paired pulse ratio (r=0.10, p=0.74; 13 neurons, 8 mice) in females. This suggests both PB CGRP and PB glutamate exert comparable effects on glutamatergic input from PB across anterior and posterior CeLC in females.

To determine if failure of neurons to potentiate results from experimental variables, we compared several experimental properties between female CeLC neurons that exhibited CGRP-dependent potentiation (>20%) and those that did not. We compared animal age (p=0.79; 16 neurons, 11 mice, Fig. 4D), viral incubation times (p=0.17; 16 neurons, 11 mice, Fig. 4E), and access resistance (p=0.44; 16 neurons, 11 mice, Fig. 4F). Experimental parameters did not differ between potentiated and non-

potentiated neurons. We also compared passive membrane properties: baseline holding current (p=0.96; 16 neurons, 11 mice, Fig. 4G), membrane resistance (p=0.40; 15 neurons, 10 mice, Fig. 4H) and cell capacitance (p=0.98; 15 neurons, 10 mice, Fig. 4I); variations in cell capacitance and resistance in particular can reflect differences in the electrical "control" of a patch and resulting resolution. Passive membrane properties did not differ between potentiated and non-potentiated neurons.

Parabrachial glutamate inputs to central amygdala show no sex differences

We considered the possibility that the sex differences in synaptic potentiation are related to sex differences in the underlying glutamatergic component of the PB_{CGRP}->CeLC signaling pathway. Figure 5A displays the location of CeLC neurons receiving glutamatergic PB_{CGRP} input. There were no sex differences in the proportion of CeLC neurons receiving PB_{CGRP} input (p=0.44; 23 female neurons, 11 mice; 21 male neurons, 10 mice, Fig. 5B); over 75% of both male and female CeLC neurons exhibited evoked oEPSCs following optic stimulation of PB_{CGRP} glutamate release. There was also no sex difference in baseline oEPSC amplitudes (p=0.95, 15 male neurons, 10 mice; 19 female neurons, 11 mice, Fig. 5C). This suggests that the strength of PB_{CGRP}->CeLC synapses is similar in males and females.

The CeLC contains a variety of GABAergic neuronal classes (Schiess et al., 1999; Xu et al., 2003; Lopez De Armentia and Sah, 2004; Chieng et al., 2006; Amano et al., 2012; Lu et al., 2015; Wilson et al., 2019). The sex differences in response to endogenous CGRP release may relate to sex difference in the subpopulations of CeLC neurons receiving direct PB_{CGRP} input. While functionally distinct central amygdala subclasses are primarily defined by their firing pattern (Schiess et al., 1999; Lopez De Armentia and Sah, 2004; Chieng et al., 2006; Amano et al., 2012; Wilson et al., 2019), subtle differences in intrinsic neuronal properties between these classes have also been observed, particularly resting membrane potential (Schiess et al., 1999; Chieng et al., 2006). We observed no sex differences in intrinsic neuron properties including holding current (p=0.27; 14 male neurons, 10 mice; 18 female neurons, 11 mice, Fig. 5D), which

313 is the current required to maintain a constant membrane potential. Similarly there was no sex difference
314 in access resistance (p=0.76, 13 male neurons, 9 mice; 17 female neurons, 12 mice, Fig. 5E) membrane
315 resistance (p=0.69; 15 male neurons, 10 mice; 17 female neurons, 12 mice, Fig. 5F), nor cell capacitance
316 (p=0.65; 15 male neurons, 10 mice; 17 female neurons, 12 mice Fig. 5G).

317

318

Discussion

Endogenous CGRP release. The central amygdala (CeLC) densely expresses a number of neuropeptides and neuropeptide receptors (Neugebauer et al., 2020). Among these is CGRP, which can increase CeLC neuronal activity in response to aversive processing, especially in chronic pain conditions (Han et al., 2005, 2010; Shinohara et al., 2017; Neugebauer et al., 2020). Previous studies used exogenously applied CGRP to reveal these effects of CGRP on CeLC neuronal functions. However, these results are confounded by the fact that both the physiological concentration and clearance rate of CGRP in CeLC are unknown. As a result, it is not known if exogenously applied CGRP mimics physiological conditions. Here, we circumvented these limitations by endogenously inducing neuropeptide release in the CeLC using optogenetics to drive parabrachial CGRP-expressing (PB_{CGRP}) activity.

High frequency firing is necessary for neuropeptide release (Schöne et al., 2014; Qiu et al., 2016). We reasoned that high frequency firing of PB_{CGRP} neurons that occurs in response to aversive stimuli (Uddin et al., 2018; Smith et al., 2023) would provide the presynaptic activity required for CGRP release. Indeed, simulating this firing by driving PB_{CGRP} neurons optogenetically resulted in release of large dense core vesicles (LDCVs) from PB_{CGRP} neurons in the central amygdala, as evidenced by imaging of LDCV sensor signals (Fig. 1F). Further, these stimuli trains resulted in potentiation of CeLC PB_{CGRP} glutamate response (Fig. 2C). That this potentiation was suppressed by a CGRP antagonist confirms it involves activation of CGRP receptors (Fig. 3B). These findings indicate that *endogenous* release of CGRP can potentiate the activity of CeLC neurons.

Sex differences. There was a sex difference in CeLC neuron response to endogenous CGRP release. Most (62%) CeLC neurons in females exhibit transient, CGRP-dependent potentiation to PB_{CGRP} glutamatergic signaling after high frequency stimulation of PB_{CGRP} inputs, compared to 13% of male neurons. In contrast, previous studies (Han et al., 2010; Okutsu et al., 2017) describe a similar level of

glutamatergic potentiation (~140%) in *male* CeLC neurons from both rats and mice with exogenous CGRP. This discrepancy might be due to lower CGRP sensitivity in males, or insufficient CGRP release to activate receptors in male CeLC neurons. This hypothesis is supported by the kinetics of CGRP-driven potentiation in male CeLC, which required >7 minutes of continuous CGRP exposure (Han et al., 2010; Okutsu et al., 2017), compared to our findings in female CeLC, where 5 seconds of CGRP release were sufficient to induce glutamate potentiation. No potentiation was observed in males even with increased PB_{CGRP} stimulation. A sex difference in CGRP sensitivity is consistent with behavioral studies demonstrating enhanced CGRP-dependent pain and anxiety-like behaviors in females (Avona et al., 2019; Paige et al., 2022), and clinical data showing greater efficacy of CGRP-targeting therapies in women (Porreca et al., 2024). CGRP antagonism in CeLC also blocks affective pain behavior exclusively in females (Presto and Neugebauer, 2022).

Sex differences in the effects of CGRP may arise from several mechanisms. CGRP clearance may be more active in males. CGRP degradation remain a field of active study (Russo and Hay, 2023), with a variety of enzymes implicated in CGRP clearance, including but not limited to matrix metalloproteinase 2 (Fernandez-Patron et al., 2000) and neutral endopeptidase (Katayama et al., 1991; Davies et al., 1992; McDowell et al., 1997). Sex differences in clearance mechanisms have been observed in some (Zhao et al., 2011; Howe et al., 2019; Omori et al., 2020), but not all studies (Reuveni et al., 2017; Bronisz et al., 2023).

Additionally, males may release less CGRP in the CeLC. PB neurons are equally activated by noxious stimuli in males and females (Smith et al., 2023), and no sex differences in LDCV release was observed *in vitro* using a novel fluorescent indicator (observation from Kim et al., 2024). However, it is possible that males either release fewer LDCVs in response to equivalent PB neuron activity, or CGRP is less densely expressed among packaged neuropeptides within LDCVs. This has not been tested, although we did not observe potentiation in males even upon increasing the hypothetical “dose” of CeLC CGRP by escalating PB_{CGRP} stimulation. Finally, considering the relatively long timescale for potentiation initiation described in males

(Han et al., 2010; Okutsu et al., 2017), it is possible that bath application of CGRP exerts its potentiating effects via signaling from an intermediate cell. CGRP receptors are robustly expressed on a variety of glial cells, including endothelial cells (Crossman et al., 1990), where they act to promote vasodilation (Brain et al., 1985). CGRP's effects on other glial types remains to be determined.

There were no sex differences in PB_{CGRP} glutamatergic input. The majority of CeLC neurons in both sexes received PB_{CGRP} glutamatergic input, in line with previous literature describing robust PB input to the "nociceptive amygdala" (Han et al., 2010; Okutsu et al., 2017). Additionally, input strength was similar between sexes, with no sex difference in the amplitude of optically evoked PB_{CGRP} glutamate currents. This suggests that low-frequency activity of PB activity, dominated by glutamate signaling, has similar effects on CeLC neurons of both sexes. However, high-frequency PB firing during chronic pain (Helassa et al., 2018; Uddin et al., 2018; Raver et al., 2020) likely shifts signaling to neuropeptide predominance. Thus, functional consequences of a sex difference in CGRP's effect in the CeLC may be restricted to aversive conditions.

Synaptic mechanisms. Short term potentiation describes transient (seconds to minutes) potentiation of glutamatergic synapses (Fioravante and Regehr, 2011), as described here in female CeLC neurons following endogenous CGRP release. A postsynaptic mechanism has been implicated in male CeLC, where CGRP engages PKA-dependent NMDA receptor recruitment to the PB_{CGRP} synapse (Han et al., 2010; Okutsu et al., 2017). Our findings are consistent with these data, as we observed no change in paired pulse ratio in female CeLC neurons following CGRP release (Fig. 3C).

Potentiation kinetics. Endogenous CGRP release transiently potentiates glutamatergic input for (~60 seconds following a 5 second stimulus train), whereas exogenous CGRP maintains potentiation at least throughout CGRP application (Han et al., 2010; Okutsu et al., 2017), and up to 30 minutes afterward (Okutsu et al., 2017). This difference in the potentiation kinetics may be due to clearance dynamics.

Endogenous CGRP release results in physiological CGRP concentrations, which are subject to clearance and diffusion away from CGRP receptors. It is possible that exogenous application of CGRP overwhelms endogenous CGRP clearance, allowing for continuous activation of CGRP receptors, and thus maintained potentiation of glutamate signaling.

Response heterogeneity. Following CGRP release, 62% of female CeLC neurons showed potentiated glutamate signaling. This heterogeneity was not explained by experimental factors such as animal age, viral incubation time, passive membrane properties, or patch access. Different CeLC regions are implicated in various functions, such as anterior/posterior CeLC activation inducing divergent behavioral/physiological responses (Bowen et al., 2020), and pain lateralizing to the right CeLC (Neugebauer and Li, 2003; Han and Neugebauer, 2004; Carrasquillo and Gereau, 2008; Ji and Neugebauer, 2009; Sadler et al., 2017; Allen et al., 2023). However, CeLC neuron location could not explain this observed heterogeneity; we found no differences in the magnitude of CGRP-dependent potentiation, nor PB_{CGRP} glutamatergic input strength, between hemispheres or across the anterior-posterior axis.

Heterogeneity in female CeLC responses may reflect the molecular diversity of CeLC GABAergic neurons. While both PKCδ and somatostatin (SST)-expressing CeLC neurons - subpopulations of CeLC GABAergic neurons - receive PB glutamatergic inputs (Wilson et al., 2019) and express CGRP receptors (Han et al., 2015; Chou et al., 2022), these populations play opposing roles in nociception (Wilson et al., 2019). It is, therefore, possible that these populations have different sensitivities to endogenous CGRP signaling. This could arise from differences in the subcellular locations of CGRP receptors relative to the site of CGRP release. Differences in the location of PB_{CGRP} terminal contacts in PKCδ and SST cells support this possibility (Shimada et al., 1989; Ye and Veinante, 2019), where perisomatic $CGRP^{+}$ terminals closely surround PKCδ-expressing CeLC neurons, but rarely SST-expressing neurons. However, these studies did not specifically investigate the location of CGRP receptors. CGRP-induced changes in proximal synapses,

413 such as those observed on PKCδ-expressing CeLC neurons, would be more easily resolved due to superior
414 voltage clamp control at synapses closer to the neuronal cell body (Spruston et al., 1993). Alternatively,
415 there could be differences in signaling downstream from the CGRP receptor; while PKA-dependent ($G\alpha_s$)
416 processes are confirmed in male neurons (Han et al., 2010; Okutsu et al., 2017), both $G\alpha_i$ and $G\alpha_q$
417 processes have been implicated in male cardiac tissue, cultured astrocytes, and immortalized cell lines
418 (Walker et al., 2010).

419 Even transient aversive PB hyperactivity induces PB neuropeptide release in the CeLC (Kim et al., 2024).
420 Our findings suggest that the female nociceptive amygdala is particularly vulnerable to excitation during
421 these CGRP release events, whereas males require sustained elevated CGRP to induce similar potentiation
422 (Han et al., 2010; Okutsu et al., 2017) . This sex difference in CGRP sensitivity may underlie sex differences
423 in affective pain processing, with females showing heightened vulnerability to pain and its related
424 affective sequalae (Mogil, 2009, 2012, 2021; Osborne and Davis, 2022).

425 References

426 Allen HN, Chaudhry S, Hong VM, Lewter LA, Sinha GP, Carrasquillo Y, Taylor BK, Kolber BJ (2023) A
427 Parabrachial-to-Amygdala Circuit That Determines Hemispheric Lateralization of Somatosensory
428 Processing. Biological Psychiatry 93:370–381 Available at:
429 https://linkinghub.elsevier.com/retrieve/pii/S0006322322015918.

430 Amano T, Amir A, Goswami S, Paré D (2012) Morphology, PKCδ expression, and synaptic responsiveness
431 of different types of rat central lateral amygdala neurons. Journal of Neurophysiology 108:3196–3205
432 Available at: https://www.physiology.org/doi/10.1152/jn.00514.2012.

433 Avona A, Burgos-Vega C, Burton MD, Akopian AN, Price TJ, Dussor G (2019) Dural Calcitonin Gene-Related
434 Peptide Produces Female-Specific Responses in Rodent Migraine Models. J Neurosci 39:4323–4331
435 Available at: https://www.jneurosci.org/lookup/doi/10.1523/JNEUROSCI.0364-19.2019.

436 Bartley EJ, Fillingim RB (2013) Sex differences in pain: a brief review of clinical and experimental findings.
437 Br J Anaesth 111:52–58.

438 Bowen AJ, Chen JY, Huang YW, Baertsch NA, Park S, Palmiter RD (2020) Dissociable control of
439 unconditioned responses and associative fear learning by parabrachial CGRP neurons. eLife 9:e59799
440 Available at: https://elifesciences.org/articles/59799.

441 Brain SD, Williams TJ, Tippins JR, Morris HR, MacIntyre I (1985) Calcitonin gene-related peptide is a potent
442 vasodilator. Nature 313:54–56 Available at: https://www.nature.com/articles/313054a0.

443 Bronisz E, Cudna A, Wierzbicka A, Kurkowska-Jastrzębska I (2023) Blood-Brain Barrier-Associated Proteins
444 Are Elevated in Serum of Epilepsy Patients. Cells 12:368 Available at: https://www.mdpi.com/2073-
445 4409/12/3/368.

446 Carrasquillo Y, Gereau RW (2008) Hemispheric Lateralization of a Molecular Signal for Pain Modulation in
447 the Amygdala. Mol Pain 4:1744-8069-4–24 Available at: http://journals.sagepub.com/doi/10.1186/1744-
448 8069-4-24 .

449 Chiang MC, Nguyen EK, Canto-Bustos M, Papale AE, Oswald A-MM, Ross SE (2020) Divergent Neural
450 Pathways Emanating from the Lateral Parabrachial Nucleus Mediate Distinct Components of the Pain
451 Response. Neuron 106:927-939.e5 Available at:
452 https://linkinghub.elsevier.com/retrieve/pii/S089662732030221X .

453 Chieng BCH, Christie MJ, Osborne PB (2006) Characterization of neurons in the rat central nucleus of the
454 amygdala: Cellular physiology, morphology, and opioid sensitivity. J Comp Neurol 497:910–927 Available
455 at: https://onlinelibrary.wiley.com/doi/10.1002/cne.21025 .

456 Chou T-M, Lee Z-F, Wang S-J, Lien C-C, Chen S-P (2022) CGRP-dependent sensitization of PKC-δ positive
457 neurons in central amygdala mediates chronic migraine. J Headache Pain 23:157 Available at:
458 https://thejournalofheadacheandpain.biomedcentral.com/articles/10.1186/s10194-022-01531-8 .

459 Crossman DC, Dashwood MR, Brain SD, McEwan J, Pearson JD (1990) Action of calcitonin gene-related
460 peptide upon bovine vascular endothelial and smooth muscle cells grown in isolation and co-culture.
461 British J Pharmacology 99:71–76 Available at:
462 https://bpspubs.onlinelibrary.wiley.com/doi/10.1111/j.1476-5381.1990.tb14656.x .

463 Davies D, Medeiros MS, Keen J, Turner AJ, Haynes LW (1992) Eosinophil Chemotactic Peptide Sequences
464 in Rat α-CGRP: Activation of a Novel Trophic Action by Neutral Endopeptidase 24.11a. Annals of the New
465 York Academy of Sciences 657:405–411 Available at:
466 https://nyaspubs.onlinelibrary.wiley.com/doi/10.1111/j.1749-6632.1992.tb22786.x .

467 de Vries Lentsch S, Rubio-Beltrán E, MaassenVanDenBrink A (2021) Changing levels of sex hormones and
468 calcitonin gene-related peptide (CGRP) during a woman's life: Implications for the efficacy and safety of
469 novel antimigraine medications. Maturitas 145:73–77.

470 Debanne D, Guérineau NC, Gähwiler BH, Thompson SM (1996) Paired-pulse facilitation and depression at
471 unitary synapses in rat hippocampus: quantal fluctuation affects subsequent release. The Journal of
472 Physiology 491:163–176 Available at:
473 https://physoc.onlinelibrary.wiley.com/doi/10.1113/jphysiol.1996.sp021204 .

474 Delaney AJ, Crane JW, Sah P (2007) Noradrenaline modulates transmission at a central synapse by a
475 presynaptic mechanism. Neuron 56:880–892.

476 Dobrunz LE, Stevens CF (1997) Heterogeneity of Release Probability, Facilitation, and Depletion at Central
477 Synapses. Neuron 18:995–1008 Available at:
478 https://linkinghub.elsevier.com/retrieve/pii/S0896627300803384 .

479 Fernandez-Patron C, Stewart KG, Zhang Y, Koivunen E, Radomski MW, Davidge ST (2000) Vascular Matrix
480 Metalloproteinase-2–Dependent Cleavage of Calcitonin Gene-Related Peptide Promotes
481 Vasoconstriction. Circulation Research 87:670–676 Available at:
482 https://www.ahajournals.org/doi/10.1161/01.RES.87.8.670 .

483 Fillingim RB (2000) Sex, gender, and pain: women and men really are different. Curr Rev Pain 4:24–30.

484 Fioravante D, Regehr WG (2011) Short-term forms of presynaptic plasticity. Current Opinion in
485 Neurobiology 21:269–274 Available at: https://linkinghub.elsevier.com/retrieve/pii/S0959438811000298.

486 Franklin KBJ, Paxinos G (2008) The mouse brain in stereotaxic coordinates, Compact 3. ed. Amsterdam
487 Heidelberg: Elsevier Academic Press.

488 Han JS, Adwanikar H, Li Z, Ji G, Neugebauer V (2010) Facilitation of Synaptic Transmission and Pain
489 Responses by CGRP in the Amygdala of Normal Rats. Mol Pain 6:1744-8069-6–10 Available at:
490 http://journals.sagepub.com/doi/10.1186/1744-8069-6-10 .

491 Han JS, Li W, Neugebauer V (2005) Critical Role of Calcitonin Gene-Related Peptide 1 Receptors in the
492 Amygdala in Synaptic Plasticity and Pain Behavior. J Neurosci 25:10717–10728 Available at:
493 https://www.jneurosci.org/lookup/doi/10.1523/JNEUROSCI.4112-05.2005 .

494 Han JS, Neugebauer V (2004) Synaptic plasticity in the amygdala in a visceral pain model in rats.
495 Neuroscience Letters 361:254–257 Available at:
496 https://linkinghub.elsevier.com/retrieve/pii/S0304394003014113 .

Han S, Soleiman MT, Soden ME, Zweifel LS, Palmiter RD (2015) Elucidating an Affective Pain Circuit that Creates a Threat Memory. Cell 162:363–374 Available at: https://linkinghub.elsevier.com/retrieve/pii/S0092867415007758 .

Helassa N, Dürst CD, Coates C, Kerruth S, Arif U, Schulze C, Wiegert JS, Geeves M, Oertner TG, Török K (2018) Ultrafast glutamate sensors resolve high-frequency release at Schaffer collateral synapses. Proc Natl Acad Sci USA 115:5594–5599 Available at: https://pnas.org/doi/full/10.1073/pnas.1720648115 .

Howe MD, Furr JW, Zhu L, Edwards NJ, McCullough LD, Gonzales NR (2019) Sex-specific Association of Matrix Metalloproteinases with Secondary Injury and Outcomes after Intracerebral Hemorrhage. Journal of Stroke and Cerebrovascular Diseases 28:1718–1725 Available at: https://linkinghub.elsevier.com/retrieve/pii/S1052305719300588 .

Janak PH, Tye KM (2015) From circuits to behaviour in the amygdala. Nature 517:284–292.

Ji G, Neugebauer V (2009) Hemispheric Lateralization of Pain Processing by Amygdala Neurons. Journal of Neurophysiology 102:2253–2264 Available at: https://www.physiology.org/doi/10.1152/jn.00166.2009 .

Kang SJ, Liu S, Ye M, Kim D-I, Pao GM, Copits BA, Roberts BZ, Lee K-F, Bruchas MR, Han S (2022) A central alarm system that gates multi-sensory innate threat cues to the amygdala. Cell Reports 40:111222 Available at: https://linkinghub.elsevier.com/retrieve/pii/S2211124722010397 .

Katayama M, Nadel JA, Bunnett NW, Di Maria GU, Haxhiu M, Borson DB (1991) Catabolism of calcitonin gene-related peptide and substance P by neutral endopeptidase. Peptides 12:563–567 Available at: https://linkinghub.elsevier.com/retrieve/pii/019697819190102U .

Kim D-I, Park S, Park S, Ye M, Chen JY, Kang SJ, Jhang J, Hunker AC, Zweifel LS, Caron KM, Vaughan JM, Saghatelian A, Palmiter RD, Han S (2024) Presynaptic sensor and silencer of peptidergic transmission

reveal neuropeptides as primary transmitters in pontine fear circuit. Cell:S0092867424007098 Available at: https://linkinghub.elsevier.com/retrieve/pii/S0092867424007098 .

Kim J, Alger BE (2001) Random Response Fluctuations Lead to Spurious Paired-Pulse Facilitation. J Neurosci 21:9608–9618 Available at: https://www.jneurosci.org/lookup/doi/10.1523/JNEUROSCI.21-24-09608.2001 .

Labastida-Ramírez A, Rubio-Beltrán E, Villalón CM, MaassenVanDenBrink A (2019) Gender aspects of CGRP in migraine. Cephalalgia 39:435–444 Available at: http://journals.sagepub.com/doi/10.1177/0333102417739584 .

Lopez De Armentia M, Sah P (2004) Firing Properties and Connectivity of Neurons in the Rat Lateral Central Nucleus of the Amygdala. Journal of Neurophysiology 92:1285–1294 Available at: https://www.physiology.org/doi/10.1152/jn.00211.2004 .

Lu Y-C, Chen Y-Z, Wei Y-Y, He X-T, Li X, Hu W, Yanagawa Y, Wang W, Wu S-X, Dong Y-L (2015) Neurochemical properties of the synapses between the parabrachial nucleus-derived CGRP-positive axonal terminals and the GABAergic neurons in the lateral capsular division of central nucleus of amygdala. Mol Neurobiol 51:105–118 Available at: http://link.springer.com/10.1007/s12035-014-8713-x .

Manabe T, Wyllie DJ, Perkel DJ, Nicoll RA (1993) Modulation of synaptic transmission and long-term potentiation: effects on paired pulse facilitation and EPSC variance in the CA1 region of the hippocampus. Journal of Neurophysiology 70:1451–1459 Available at: https://www.physiology.org/doi/10.1152/jn.1993.70.4.1451 .

Mazzitelli M, Marshall K, Pham A, Ji G, Neugebauer V (2021) Optogenetic Manipulations of Amygdala Neurons Modulate Spinal Nociceptive Processing and Behavior Under Normal Conditions and in an Arthritis Pain Model. Front Pharmacol 12:668337.

McDowell G, Coutie W, Shaw C, Buchanan KD, Struthers AD, Nicholls DP (1997) The effect of the neutral endopeptidase inhibitor drug, candoxatril, on circulating levels of two of the most potent vasoactive peptides. Brit J Clinical Pharma 43:329–332 Available at: https://bpspubs.onlinelibrary.wiley.com/doi/10.1046/j.1365-2125.1997.00545.x .

Mogil JS (2009) Animal models of pain: progress and challenges. Nat Rev Neurosci 10:283–294.

Mogil JS (2012) Sex differences in pain and pain inhibition: multiple explanations of a controversial phenomenon. Nat Rev Neurosci 13:859–866.

Mogil JS (2021) Sources of Individual Differences in Pain. Annu Rev Neurosci 44:1–25.

Neugebauer V (2015) Amygdala pain mechanisms. Handb Exp Pharmacol 227:261–284.

Neugebauer V, Li W (2003) Differential Sensitization of Amygdala Neurons to Afferent Inputs in a Model of Arthritic Pain. Journal of Neurophysiology 89:716–727 Available at: https://www.physiology.org/doi/10.1152/jn.00799.2002 .

Neugebauer V, Li W, Bird GC, Bhave G, Gereau RW (2003) Synaptic plasticity in the amygdala in a model of arthritic pain: differential roles of metabotropic glutamate receptors 1 and 5. J Neurosci 23:52–63.

Neugebauer V, Mazzitelli M, Cragg B, Ji G, Navratilova E, Porreca F (2020) Amygdala, neuropeptides, and chronic pain-related affective behaviors. Neuropharmacology 170:108052.

Okutsu Y, Takahashi Y, Nagase M, Shinohara K, Ikeda R, Kato F (2017) Potentiation of NMDA receptor-mediated synaptic transmission at the parabrachial-central amygdala synapses by CGRP in mice. Mol Pain 13:174480691770920 Available at: http://journals.sagepub.com/doi/10.1177/1744806917709201 .

Omori W, Hattori K, Kajitani N, Okada-Tsuchioka M, Boku S, Kunugi H, Okamoto Y, Takebayashi M (2020) Increased Matrix Metalloproteinases in Cerebrospinal Fluids of Patients With Major Depressive Disorder

and Schizophrenia. International Journal of Neuropsychopharmacology 23:713–720 Available at: https://academic.oup.com/ijnp/article/23/11/713/5872125 .

Osborne NR, Davis KD (2022) Sex and gender differences in pain. Int Rev Neurobiol 164:277–307.

Paige C, Plasencia-Fernandez I, Kume M, Papalampropoulou-Tsiridou M, Lorenzo L-E, David ET, He L, Mejia GL, Driskill C, Ferrini F, Feldhaus AL, Garcia-Martinez LF, Akopian AN, De Koninck Y, Dussor G, Price TJ (2022) A Female-Specific Role for Calcitonin Gene-Related Peptide (CGRP) in Rodent Pain Models. J Neurosci 42:1930–1944 Available at: https://www.jneurosci.org/lookup/doi/10.1523/JNEUROSCI.1137-21.2022 .

Porreca F, Navratilova E, Hirman J, Van Den Brink AM, Lipton RB, Dodick DW (2024) Evaluation of outcomes of calcitonin gene-related peptide (CGRP)-targeting therapies for acute and preventive migraine treatment based on patient sex. Cephalalgia 44:03331024241238153 Available at: https://journals.sagepub.com/doi/10.1177/03331024241238153 .

Presto P, Neugebauer V (2022) Sex Differences in CGRP Regulation and Function in the Amygdala in a Rat Model of Neuropathic Pain. Front Mol Neurosci 15:928587 Available at: https://www.frontiersin.org/articles/10.3389/fnmol.2022.928587/full .

Qiu J, Nestor CC, Zhang C, Padilla SL, Palmiter RD, Kelly MJ, Rønnekleiv OK (2016) High-frequency stimulation-induced peptide release synchronizes arcuate kisspeptin neurons and excites GnRH neurons. eLife 5:e16246 Available at: https://elifesciences.org/articles/16246 .

Raver C, Uddin O, Ji Y, Li Y, Cramer N, Jenne C, Morales M, Masri R, Keller A (2020) An Amygdalo-Parabrachial Pathway Regulates Pain Perception and Chronic Pain. J Neurosci 40:3424–3442 Available at: https://www.jneurosci.org/lookup/doi/10.1523/JNEUROSCI.0075-20.2020 .

582 Reuveni G, Golderman V, Shavit-Stein E, Rosman Y, Shrot S, Chapman J, Harnof S (2017) Measuring
583 thrombin activity in frozen brain tissue. NeuroReport 28:1176–1179 Available at:
584 https://journals.lww.com/00001756-201712020-00012 .

585 Russo AF, Hay DL (2023) CGRP physiology, pharmacology, and therapeutic targets: migraine and beyond.
586 Physiological Reviews 103:1565–1644 Available at:
587 https://journals.physiology.org/doi/10.1152/physrev.00059.2021 .

588 Sadler KE, McQuaid NA, Cox AC, Behun MN, Trouten AM, Kolber BJ (2017) Divergent functions of the left
589 and right central amygdala in visceral nociception. Pain 158:747–759 Available at:
590 https://journals.lww.com/00006396-201704000-00021 .

591 Schiess MC, Callahan PM, Zheng H (1999) Characterization of the electrophysiological and morphological
592 properties of rat central amygdala neurons in vitro. J Neurosci Res 58:663–673.

593 Schöne C, Apergis-Schoute J, Sakurai T, Adamantidis A, Burdakov D (2014) Coreleased Orexin and
594 Glutamate Evoke Nonredundant Spike Outputs and Computations in Histamine Neurons. Cell Reports
595 7:697–704 Available at: https://linkinghub.elsevier.com/retrieve/pii/S2211124714002526 .

596 Schwaber JS, Sternini C, Brecha NC, Rogers WT, Card JP (1988) Neurons containing calcitonin gene-related
597 peptide in the parabrachial nucleus project to the central nucleus of the amygdala. J Comp Neurol
598 270:416–426, 398–399.

599 Shimada S, Inagaki S, Kubota Y, Kito S, Funaki H, Takagi H (1989) Light and electron microscopic studies of
600 calcitonin gene-related peptide-like immunoreactive terminals in the central nucleus of the amygdala and
601 the bed nucleus of the stria terminalis of the rat. Exp Brain Res 77 Available at:
602 http://link.springer.com/10.1007/BF00250584 .

603 Shimada S, Shiosaka S, Emson PC, Hillyard CJ, Girgis S, MacIntyre I, Tohyama M (1985) Calcitonin gene-
604 related peptidergic projection from the parabrachial area to the forebrain and diencephalon in the rat: an
605 immunohistochemical analysis. Neuroscience 16:607–616.

606 Shinohara K, Watabe AM, Nagase M, Okutsu Y, Takahashi Y, Kurihara H, Kato F (2017) Essential role of
607 endogenous calcitonin gene-related peptide in pain-associated plasticity in the central amygdala. Eur J
608 Neurosci 46:2149–2160 Available at: https://onlinelibrary.wiley.com/doi/10.1111/ejn.13662 .

609 Smith JA, Ji Y, Lorsung R, Breault MS, Koenig J, Cramer N, Masri R, Keller A (2023) Parabrachial Nucleus
610 Activity in Nociception and Pain in Awake Mice. J Neurosci 43:5656–5667.

611 Spruston N, Jaffe DB, Williams SH, Johnston D (1993) Voltage- and space-clamp errors associated with the
612 measurement of electrotonically remote synaptic events. Journal of Neurophysiology 70:781–802
613 Available at: https://www.physiology.org/doi/10.1152/jn.1993.70.2.781 .

614 Stratton H, Lee G, Dolatyari M, Ghetti A, Cotta T, Mitchell S, Yue X, Ibrahim M, Dumaire N, Salih L, Moutal
615 A, François-Moutal L, Martin L, Navratilova E, Porreca F (2024) Nociceptors are functionally male or
616 female: from mouse to monkey to man. Brain:awae179 Available at:
617 https://academic.oup.com/brain/advance-article/doi/10.1093/brain/awae179/7686987 .

618 Tallent MK (2008) Presynaptic Inhibition of Glutamate Release by Neuropeptides: Use-Dependent
619 Synaptic Modification. In: Inhibitory Regulation of Excitatory Neurotransmission (Darlison MG, ed), pp
620 177–200 Results and Problems in Cell Differentiation. Berlin, Heidelberg: Springer Berlin Heidelberg.
621 Available at: http://link.springer.com/10.1007/400_2007_037 .

622 Ting JT, Daigle TL, Chen Q, Feng G (2014) Acute Brain Slice Methods for Adult and Aging Animals:
623 Application of Targeted Patch Clamp Analysis and Optogenetics. In: Patch-Clamp Methods and Protocols

(Martina M, Taverna S, eds), pp 221–242 Methods in Molecular Biology. New York, NY: Springer New York. Available at: https://link.springer.com/10.1007/978-1-4939-1096-0_14 .

Uddin O, Studlack P, Akintola T, Raver C, Castro A, Masri R, Keller A (2018) Amplified parabrachial nucleus activity in a rat model of trigeminal neuropathic pain. Neurobiology of Pain 3:22–30 Available at: https://linkinghub.elsevier.com/retrieve/pii/S2452073X17300284 .

Walker CS, Conner AC, Poyner DR, Hay DL (2010) Regulation of signal transduction by calcitonin gene-related peptide receptors. Trends in Pharmacological Sciences 31:476–483 Available at: https://linkinghub.elsevier.com/retrieve/pii/S0165614710001124 .

Wilson TD, Valdivia S, Khan A, Ahn H-S, Adke AP, Martinez Gonzalez S, Sugimura YK, Carrasquillo Y (2019) Dual and Opposing Functions of the Central Amygdala in the Modulation of Pain. Cell Reports 29:332-346.e5 Available at: https://linkinghub.elsevier.com/retrieve/pii/S221112471931188X .

Xu W, Lundeberg T, Wang YT, Li Y, Yu L-C (2003) Antinociceptive effect of calcitonin gene-related peptide in the central nucleus of amygdala: activating opioid receptors through amygdala–periaqueductal gray pathway. Neuroscience 118:1015–1022 Available at: https://linkinghub.elsevier.com/retrieve/pii/S0306452203000691 .

Ye J, Veinante P (2019) Cell-type specific parallel circuits in the bed nucleus of the stria terminalis and the central nucleus of the amygdala of the mouse. Brain Struct Funct 224:1067–1095 Available at: http://link.springer.com/10.1007/s00429-018-01825-1 .

Zhao L, Yao J, Mao Z, Chen S, Wang Y, Brinton RD (2011) 17β-Estradiol regulates insulin-degrading enzyme expression via an ERβ/PI3-K pathway in hippocampus: Relevance to Alzheimer's prevention. Neurobiology of Aging 32:1949–1963 Available at: https://linkinghub.elsevier.com/retrieve/pii/S0197458009004023 .

Figure legends

Figure 1. Low frequency optic stimulation of PB_{CGRP} terminals in CeLC induces glutamate release, while high frequency optic stimulation induces neuropeptide release. (A) AAV5-DIO-ChR2-eYFP OR AAV5-DIO-ChR2-eYFP AND AAVDJ-DIO-CYbSEP2 virus was injected into the left or right lateral parabrachial of CGRP-Cre mice. CeLC slices were collected for either fiber photometry or voltage clamp patch electrophysiology. (B) Photomicrographs showing PB_{CGRP} EYFP+ terminals in ipsilateral central amygdala (CeLC). Scale bar = 200 µm. A biocytin filled CeLC neuron shown in inset. Scale bar = 20 µm. (C) An injection site, with dense eYFP+ PB_{CGRP} neuronal cell bodies located in lateral parabrachial (LPB). Scale bar = 200 µm. SCP = superior cerebellar peduncle. (D) A single optic stimulus induces an optically evoked EPSC (oEPSC) at baseline (black trace) which is suppressed by 20 µM CNQX (red). Blue arrow indicates delivery of single optic stimulus (3 msec duration). (E) Rapid reduction in oEPSC amplitudes during delivery of a high frequency optic tetanus. Example stimulus train and response in CeLC neuron shown in inset (cyan). (F) Heat map depicting the change in CybSEP2 fluorescence (ΔF/F) in response to different durations of 20 Hz stimulus train of ChR2-expressing PB_{CGRP} inputs in a male CeLC slice. Three trials averaged per row. (G) Quantification of average fluorescence in 5 seconds pre and post stimulus for trials shown in F.

Figure 2. Optic stimulation of PB CGRP induces a transient, CGRP-dependent potentiation of glutamate sensitivity, preferentially in females. PB_{CGRP} neurotransmitter release was induced via single (glutamate) or high frequency (CGRP) optic tetanus. oEPSCs evoked by single-pulse optic stimulation from CeLC neurons from a female(**A**) and a male (**B**) neuron recorded at baseline (black traces) and post PB CGRP release (red traces). Note the potentiation in the female, but not the male neuron. Blue arrows indicate delivery of single optic stimulus (3 msec duration). (**C**)

668 Amplitudes of optically evoked PB_{CGRP} glutamate responses (oEPSC) in the 80 second period
669 following high frequency optic in female and male CeLC neurons. Dashed lines depict averages.
670 (**D**) Amplitude of oEPSC, normalized to baseline, transiently potentiated for ~60 seconds in
671 female CeLC neurons (pink). (**E**) A shift in baseline holding current specifically in females
672 accompanied this high frequency optic stimulus. Using a higher frequency optical train to
673 enhance PB CGRP release (20 Hz, 10 sec) and recording in 0 mg solution to enhance NMDA
674 currents failed to evoke oEPSC potentiation (**F,G**). (**H**) Significant difference in the effects of
675 endogenous CGRP release on female and male neurons. Increases and decreases were defined
676 as >20% change in oEPSC amplitudes.

677 **Figure 3. Potentiation is CGRP-dependent and influences presynaptic release probability in**
678 **females.** (**A**) Potentiation of PB_{CGRP} glutamate signaling in female neurons is reproducible, as a
679 second PB CGRP release event ($CGRP_2$) induces a similar level of potentiation as an initial PB
680 CGRP release event ($CGRP_1$). (**B**) This potentiation is CGRP-dependent as evidenced by its
681 suppression by 1 µM CGRP8-37, CGRP receptor antagonist. (**C**) The potentiation is not associated
682 in with a change in paired pulse ratios, indicating that it does not involve presynaptic
683 mechanisms. Black dashed lines indicate group averages. Inset shows traces of paired pulses
684 (100 msec interstimulus interval) at baseline (black) and after high frequency optic tetanus (red).

685 **Figure 4. CGRP-dependent potentiation and input strength is not lateralized, and response to**
686 **CGRP is not due to experimental variables.** All data from female CeLC neurons. Potentiation is
687 indistinguishable in neurons in the left or right CeLC (**A**). Two measures of PB_{CGRP} glutamatergic
688 input strength, oEPSC baseline amplitudes (**B**) and paired pulse ratios at baseline (**C**) also show
689 no lateralization. Potential experimental sources of heterogeneity are not correlated with

690 potentiation – animal age (**D**); virus incubation time (**E**) do not differ between responder neurons
691 (>20% potentiation) and non-responder neurons. Similarly, access resistance (**F**), baseline
692 current (**G**), membrane resistance (**H**) or cell capacitance (**I**) show no difference between
693 responders and non-responders.

694 **Figure 5. Male and female CeLC neurons recording locations and membrane properties** (**A**)
695 Location of male (blue) and female (pink) CeLC neurons that received direct PB_{CGRP} glutamatergic
696 input recorded in the lateral capsule of the CeLC across a number of coronal slices. Positions
697 indicated relative to bregma. (**B**) There was no sex difference in the proportion of recorded CeLC
698 neurons that received direct PB_{CGRP} glutamatergic input. (**C**) There was no sex difference in
699 oEPSC amplitudes at baseline, a metric of input strength. Male and female CeLC neurons also
700 had similar baseline currents (**D**), access resistance (**E**), membrane resistance (**F**), or membrane
701 capacitance (**G**).

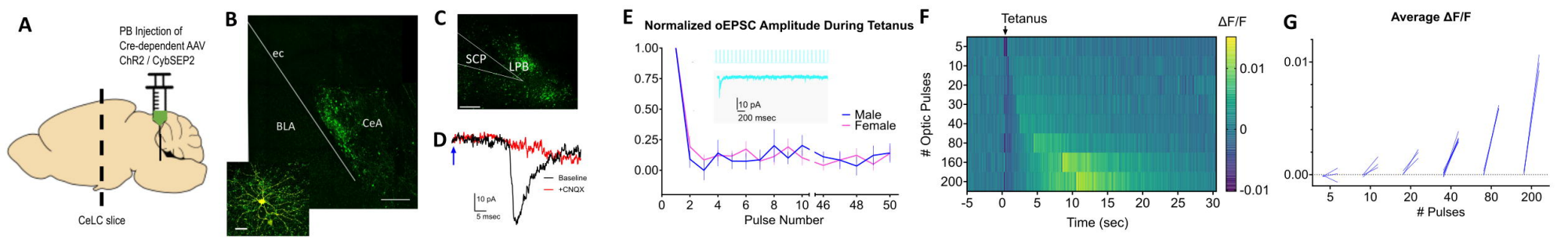
A
PB Injection of
Cre-dependent AAV
ChR2 / CybSEP2
CeLC slice
B
ec
BLA
CeA
C
SCP
LPB
D
10 pA
5 msec
Baseline
+CNQX
E
Normalized oEPSC Amplitude During Tetanus
1.00
0.75
0.50
0.25
0.00
10 pA
200 msec
Male
Female
0
2
4
6
8
10
46
48
50
Pulse Number
F
Tetanus
ΔF/F
Optic Pulses
5
10
20
30
40
80
160
200
0.01
0
-0.01
-5
0
5
10
15
20
25
30
Time (sec)
G
Average ΔF/F
0.01
0.00
5
10
20
40
80
200
Pulses

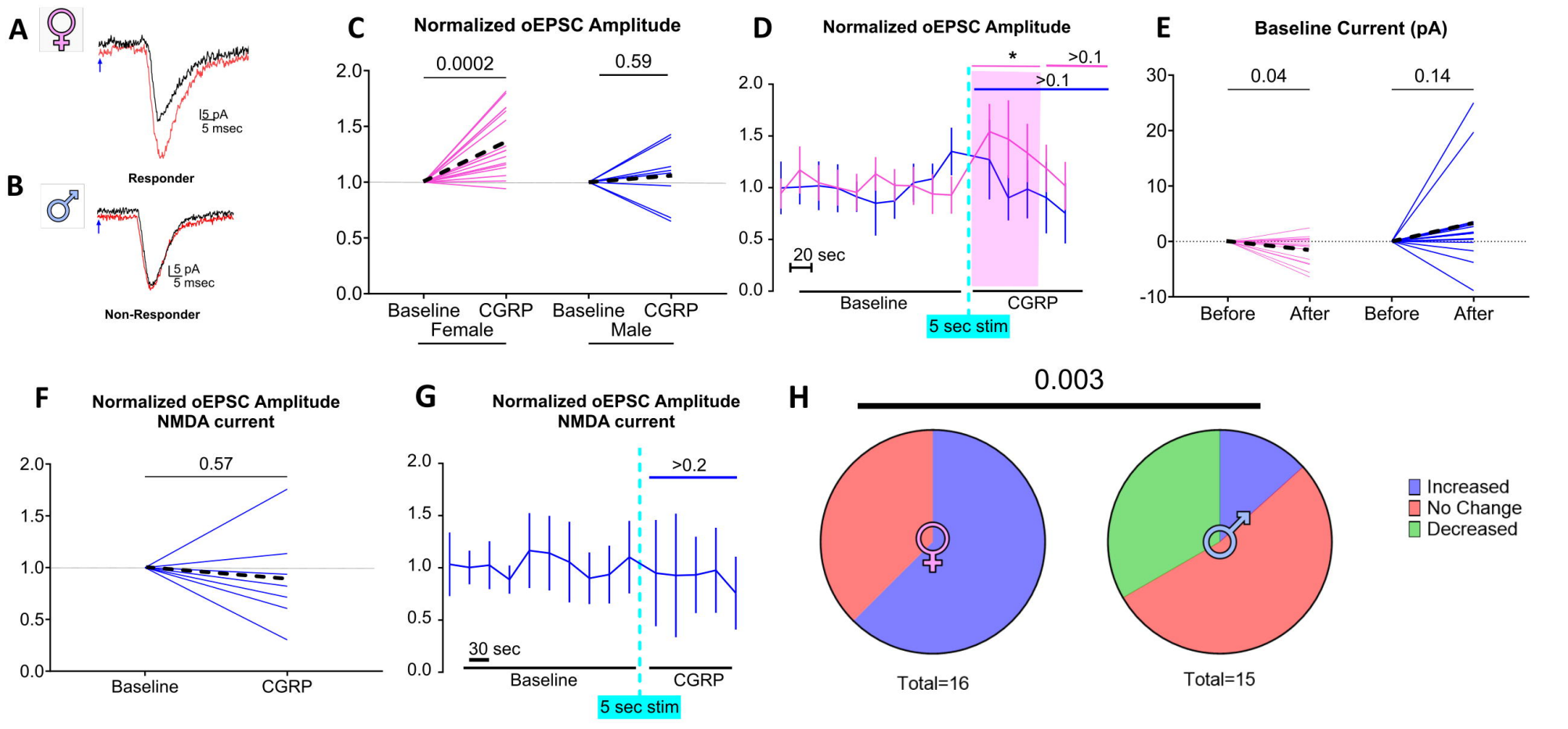
A
5 pA
5 msec
Responder
B
5 pA
5 msec
Non-Responder
C
Normalized oEPSC Amplitude
0.0002
0.59
2.0
1.5
1.0
0.5
0.0
Baseline
CGRP
Female
Baseline
CGRP
Male
D
Normalized oEPSC Amplitude
*
>0.1
>0.1
20 sec
Baseline
CGRP
5 sec stim
E
Baseline Current (pA)
0.04
0.14
30
20
10
0
-10
Before
After
Before
After
F
Normalized oEPSC Amplitude
NMDA current
0.57
Baseline
CGRP
G
Normalized oEPSC Amplitude
NMDA current
>0.2
30 sec
Baseline
CGRP
5 sec stim
H
0.003
Total=16
Total=15
Increased
No Change
Decreased

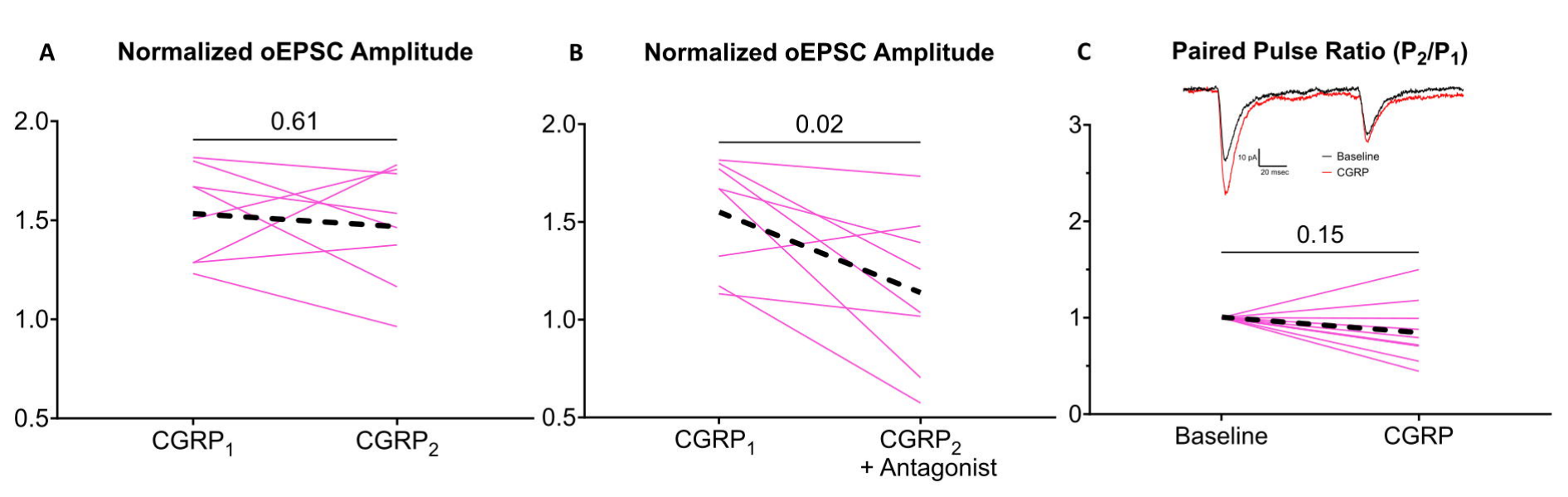
A
Normalized oEPSC Amplitude
0.61
2.0
1.5
1.0
0.5
CGRP1
CGRP2
B
Normalized oEPSC Amplitude
0.02
2.0
1.5
1.0
0.5
CGRP1
CGRP2
+ Antagonist
C
Paired Pulse Ratio (P2/P1)
10 pA
20 msec
Baseline
CGRP
0.15
3
2
1
0
Baseline
CGRP

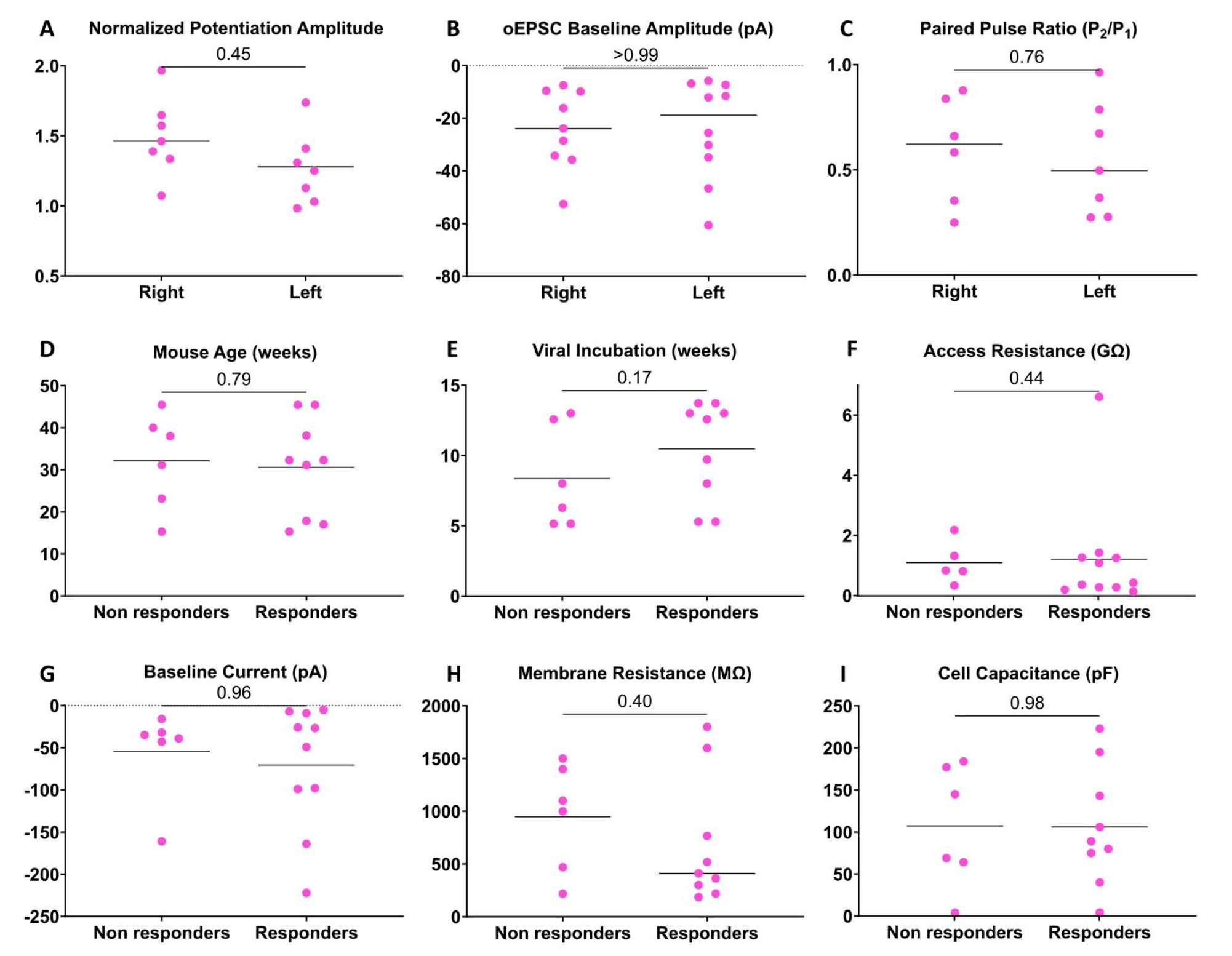
A
Normalized Potentiation Amplitude
0.45
2.0
1.5
1.0
0.5
Right
Left
B
oEPSC Baseline Amplitude (pA)
>0.99
0
-20
-40
-60
-80
Right
Left
C
Paired Pulse Ratio (P_2/P_1)
0.76
1.0
0.5
0.0
Right
Left
D
Mouse Age (weeks)
0.79
50
40
30
20
10
0
Non responders
Responders
E
Viral Incubation (weeks)
0.17
15
10
5
0
Non responders
Responders
F
Access Resistance (GΩ)
0.44
6
4
2
0
Non responders
Responders
G
Baseline Current (pA)
0.96
0
-50
-100
-150
-200
-250
Non responders
Responders
H
Membrane Resistance (MΩ)
0.40
2000
1500
1000
500
0
Non responders
Responders
I
Cell Capacitance (pF)
0.98
250
200
150
100
50
0
Non responders
Responders

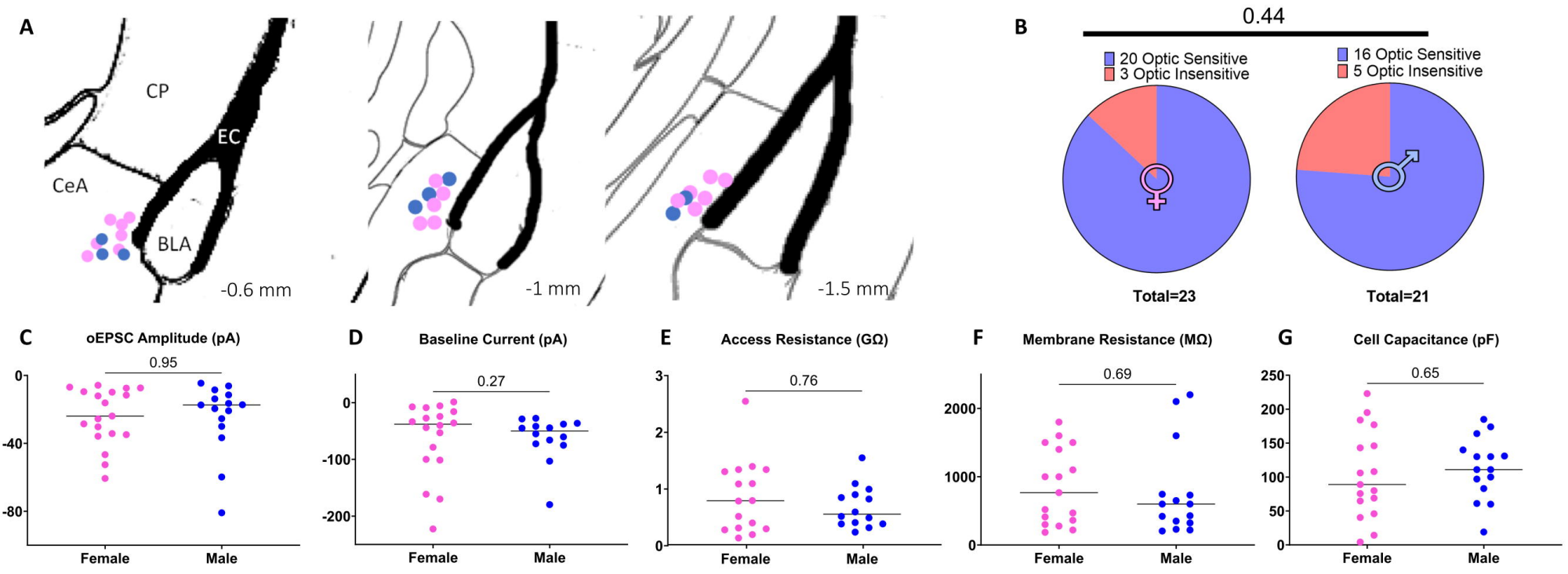
A
CP
EC
CeA
BLA
-0.6 mm
-1 mm
-1.5 mm
B
0.44
20 Optic Sensitive
3 Optic Insensitive
16 Optic Sensitive
5 Optic Insensitive
Total=23
Total=21
C
oEPSC Amplitude (pA)
0.95
0
-40
-80
Female
Male
D
Baseline Current (pA)
0.27
0
-100
-200
Female
Male
E
Access Resistance (GΩ)
0.76
3
2
1
0
Female
Male
F
Membrane Resistance (MΩ)
0.69
2000
1000
0
Female
Male
G
Cell Capacitance (pF)
0.65
250
200
150
100
50
0
Female
Male